Selective CO_2 Gas Sensor via Noble Metal Functionalized Nano MoO_3: NiO

M.V. Manasa[1,2], G. Sarala Devi[1,2] and P.S. Prasada Reddy[3]*
[1]Polymer and Functional Materials Division, CSIR-Indian Institute of Chemical Technology (CSIR-IICT), Habsiguda, Hyderabad – 500007
[2]Academy of Scientific and Innovative Research (AcSIR), CSIR-IICT Campus, Habsiguda, Hyderabad-500007
[3]Department of Physics, Dr. B.R. Ambedkar University, Andhra Pradesh-532001
Email Id: sarala@csiriict.in, sarala.ipc@gmail.com; Ph: +91-40-27191532

Abstract: The nano structured architectures of metal oxides have unique and highly attractive properties like high surface-to-volume ratio, high bandgap, low particle size, etc. In the present work we report the design & synthesis of novel p-n type semiconducting Ag incorporated MoO_3: NiO (MNA) nanocomposite as Carbon dioxide (CO_2) gas sensor, which demonstrated an efficient conductivity and superior stability through nano structured engineering. Ag-loaded MoO_3: NiO sensor showed excellent sensitivity (S= 87.64%) and selectivity towards CO_2 gas compared to MoO_3: NiO (MN) sensor which exhibited low sensitivity of S=68.5%. A plausible gas sensing mechanism was deduced in terms of adsorption – desorption phenomena. The results explicitly confirm the effectiveness of MNA nanocomposite engineered for development of high performance CO_2 gas sensor.

Keywords: MoO_3: NiO nanocomposite, XRD, Particle size Analyzer, XPS and CO_2 Sensor.

I. INTRODUCTION

Semiconductor materials have been used to improve the performance of downscaling electronic systems, with the increasing requirements of efficiency, functionality, cost and portability of the electronic devices [1-3]. This downscaling of devices has driven the electronics industry towards nano world and evoked the research of various nanomaterials such as nanoparticles, quantum dots, one-dimensional (1D) nanotubes, two-dimensional (2D) thin films, etc. which has emerged as promising options due to their superior electrical and mechanical properties [4-7]. The semiconductor nanomaterials also allow the fabrication of more efficient devices as they have the ability of band gap tuning with the change in particle size. At the same time their high surface to volume ratio combined with their excellent electrical properties has rendered them as building blocks for the development of robust and highly sensitive gas sensors [8-14].

MoO_3 exhibits in three forms orthorhombic (α-MoO_3), monoclinic (β-MoO_3) and hexagonal (h-MoO_3) among which α-MoO_3 is found to be thermodynamically stable due to its excellent physicochemical properties [15-18]. Among several n-type semiconducting nano metal oxides like ZnO, SnO_2, TiO_2, etc., MoO_3 was found to be better candidate for gas sensing performance comparatively due to the presence of more number of unpaired electrons and high band gap of 3.6eV [19-21].

Nickel oxide (NiO) is an important transition metal oxide with cubic lattice structure exhibiting anodic electro-chromism, excellent durability and electrochemical stability, large spin optical density and various manufacturing possibilities with potential use in a variety of applications such as catalysis, battery cathodes, gas sensors, electrochromic films, magnetic materials, dye sensitized photo-cathodes [22-29]. Among several p-type semiconducting materials like CuO, CdO, SnO, Zr_2O_3, etc., nano NiO has higher number of holes providing a high probability of producing free unpaired electrons when incorporated in nano MoO_3 [30-32].

There are numerous reports on gas sensors for H_2, EtOH, monohydrate vapours, etc., there are not many literature reported on nanostructured materials for CO_2 gas sensing. Z.Y.Can et al reported the application of bulk ZnO for CO_2 gas sensing which exhibited a sensitivity of 37.8% at an operating temperature of 250^{o}C [33]. N.O.Savage et al reported a high temperature potentiometric CO_2 gas sensor with sensitivity of 29% [34].

In the present study we describe the gas sensing characteristics of MoO_3:NiO nanomaterials (synthesized via Hydrothermal protocol which has unique advantages in terms of high reactivity of reactants and easy control of interface reactions and enables to produce stable material) towards CO_2 gas, and further, four main factors affecting the gas sensing properties i.e., sensitivity, selectivity, stability and response-recovery time which depends upon the activation energy and effective charge transfer process in the interfaces of MoO_3: NiO nanocomposite were considered. Since the addition of a noble metal compels the reaction between the surface of the nanocomposite and gas molecules, an optimized wt% of noble metal (Ag) was incorporated in MoO_3: NiO nanocomposite aiming to develop suitable CO_2 gas sensor materials of higher sensitivity and selectivity.

II. EXPERIMENTAL

Synthesis of molybdenum oxide (MoO_3) and nickel oxide (NiO) nanoparticles were carried out via hydrothermal protocol. In a typical synthesis, 1M PEG was mixed with 100ml D.I. water under continuous magnetic stirring till a clear solution was formed. To this solution, 2M of ammonium molybdate ($(NH_4)_6Mo_7O_{24}$) was added under continuous stirring for 4h to obtain the desired reactant mixture during which the solution changed to grey colour. The solution was transferred into Teflon coated autoclave, set at 150^{o}C and processed for 4h after which the reaction vessel was cooled, the obtained precipitate was collected, centrifuged at 4000ppm, oven dried at 80^{o}C/3h and pulverized to obtain fine and homogeneous material. The obtained material was calcined at 400^{o}C for 2h to eliminate the expected contaminants [35].

Similar procedure was adopted for synthesis of NiO nanoparticles where 3M PEG and 2M nickel acetate ($Ni(CH_3COO)_2$) were taken as reactants. To synthesize MoO_3: NiO (MN) nano composite, 1wt% of nano NiO (0.01g) was impregnated into the synthesized MoO_3 nanoparticles. Thereafter, 0.1wt% of Ag (0.001g) was impregnated into MN to obtain MoO_3: NiO: Ag (MNA) nanocomposite. The synthesized nanomaterials were characterized and gas sensing studies were carried out towards CO_2 gas.

III. EQUIPMENT USED FOR CHARACTERIZATION OF SYNTHESIZED MNA NANOPARTICLES

X-ray powder diffraction data was recorded on Siemens (D5000) diffractometer using Cu Kα radiation (λ = 1.5406 A°) in the range of 2θ = 20–80^o. Particle size was recorded by particle size analyzer Horiba SZ100 and the morphological analysis of the samples was carried out by transmission electron microscopy (TEM) on TEM-TALOS L120C model. UV-Vis DRS was recorded by Perkin Elmer U-2910 UV double beam spectroscopy. X-Ray Fluorescence (XRF) was recorded on OCEAN PUMA 7600D spectrometer.

IV. FABRICATION OF THE SENSOR ELEMENT

The substance used for the fabrication of the sensor element was alumina tube of 10 mm length, having two silver electrodes on either side separated by 6 mm, 5 mm external diameter and 3 mm internal diameter. For chemical sensor application, the sensor materials were mixed and ground with D.I. water in an agate mortar to form a paste, then the resulting paste was coated on an alumina tube substrate having a pair of silver electrodes on either side followed by drying and calcination at 400°C for 2h. Finally, a Ni–Cr heating wire was inserted into the tube to heat the sensor. The resulting sensor element was subjected to measurements of the electrical resistance in presence and absence of CO_2 gas

in air. The operating temperature and concentrations of CO_2 gas were varied in order to establish maximum sensor response. For the resistance measurements the sensor element was placed on a temperature-controlled tungsten coil heater inside the enclosure. A load resistor R_L was connected in series with the sensor element Rs. A chromel–alumel thermocouple (TC) was placed on the device to indicate the operating temperature.

The sensitivity (S), defined as the ratio $S=\Delta R/R_a$, where R_a and R_g are the sensor resistance in air and in test gas, respectively, ΔR is the difference between R_a and R_g. The response time is defined as the time required for the variation in conductance to reach 90% of the equilibrium value after which a test gas is injected. The recovery time is the time taken for the sensor to return to its original conductance state in air.

V. Results and Discussion

A. *X-Ray Diffraction (XRD)*

The XRD pattern of the synthesized MoO_3 nanoparticles, MN & MNA nanocomposites is as shown in the figure 1(a-c). The (1 0 1), (4 0 0), (2 1 0), (0 1 1), (2 1 1), (0 2 0), (1 2 1), (2 2 1) & (7 0 2) planes correspond to MoO_3 which are incoherence with the JCPDS data (no. 897112) with lattice constants a=13.85A^o, b=3.69A^o, c=3.96A^o and lattice angles α=β=γ=90^o. The (1 0 4) plane correspond to NiO (JCPDS data no. 897390) with lattice constants a=b=2.95A^o, c=7.22A^o and lattice angles α=β=γ=90^o whereas (2 0 0) plane corresponds to Ag (JCPDS data no. 652870). The average crystallite size (D) of the synthesized nanomaterials were calculated using the following Scherrer's formula,

$$D = \frac{K.\lambda}{\beta.Cos\theta} \qquad (1)$$

Where K indicates the Scherrer's constant (0.9), λ is the wavelength of X-Ray (1.54A^o), β indicates the full width half maximum of each peak in respective XRD pattern and θ indicates the Bragg's angle of diffraction.

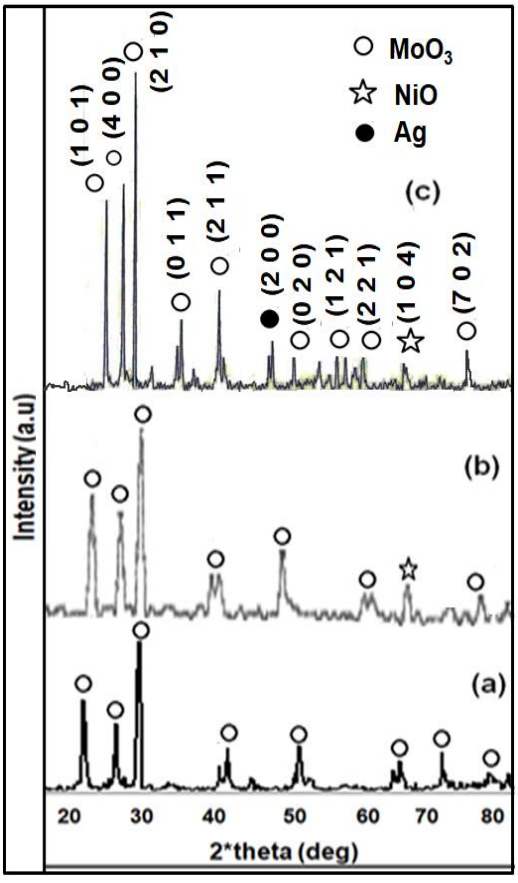

Fig. 1 XRD pattern of (a) MoO_3 (b) MN & (c) MNA nanocomposites

The crystallite size of synthesized nano MoO_3 MN & MNA nanocomposites is calculated as 14.26nm, 22.17nm & 15.14nm respectively.

B. Particle Size Analysis (PSA)

The particle size distribution of synthesized MoO_3 nanoparticles, MN & MNA nanocomposites are as shown in figure 2(a-c). The mean particle size of MoO_3 nanoparticles, MN and MNA nanocomposites are observed as 24.8nm, 24.5nm and 19nm respectively. The observed particle sizes are incoherence with the respective XRD data. A decrease in particle size was observed on incorporation of noble metal, this may be because the noble metallic nanoparticles are demonstrated as promising hyper-thermic agents and by heating of metallic nanoparticles it forms a magnetic field. This oscillating magnetic field produces electric current through which heat is generated. The heat generation occurs due to eddy current which dissipates into the surrounding from nanoparticles causing thermal ablation resulting in decrease in particle size [13].

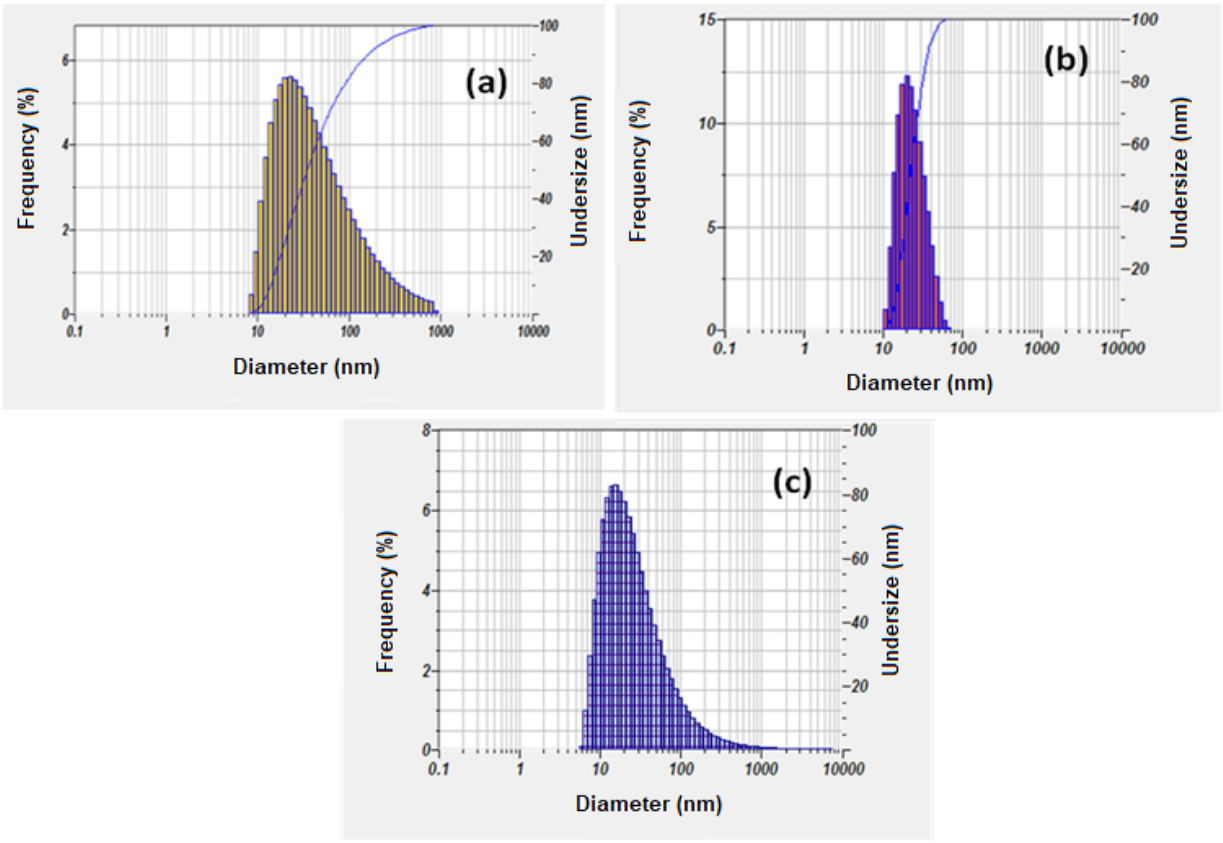

Fig. 2 Particle Size Distribution of (a) MoO_3 nanoparticles (b) MN & (c) MNA nanocomposites

C. Transmission Electron Microscopy (TEM)

The TEM micrograph and SAED pattern of MNA nanocomposite are shown in figure3(a,b) which clearly reveals the orthorhombic structure of MoO_3 & black spherical structure of NiO where as the spherical shape particles attached to the surface of MoO_3/NiO may be attributed to Ag as seen in figure 3(a). The selected area electron diffraction (SAED) pattern illustrates spot patterns designating the crystalline nature of the material (figure 3(b)).

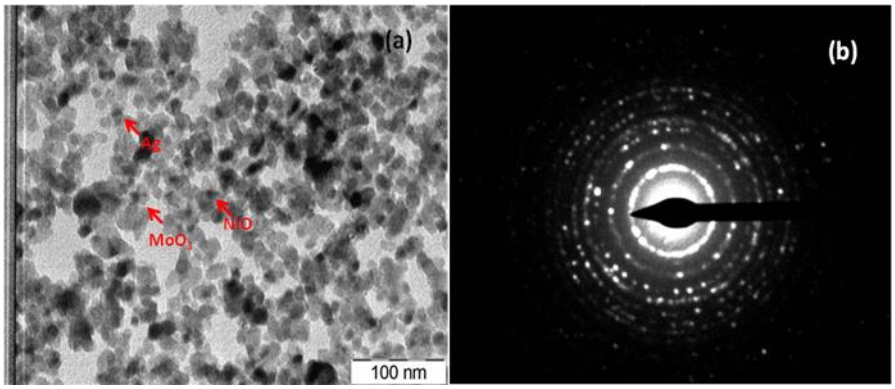

Fig. 3 (a) TEM micrograph & (b) SAED pattern of MNA nanocomposite

D. X-Ray Fluorescence Spectroscopy (XRF)

The XRF spectra of synthesized MoO_3 nanoparticles, MN & MNA nanocomposites are given in figure 4(a-c). The spectra confirm the presence of Mo, Ni, O & Ag signal in the samples without any impurities.

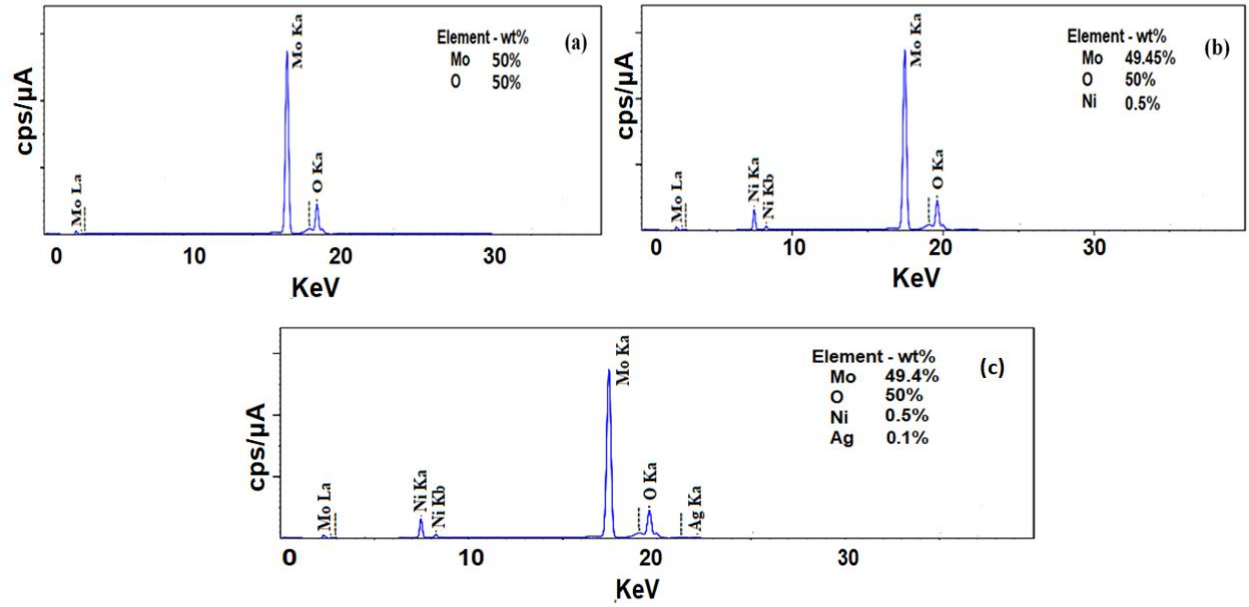

Fig. 4 XRF spectra of (a) MoO_3 nanoparticles, (b) MN & (c) MNA nanocomposites

E. UV-Visible Spectroscopy (UV-Vis)

Figure 5(a-c) shows the Tauc plots and corresponding UV-DRS spectra of MoO_3, MN & MNA nanocomposites. The optical properties of MoO_3 nanoparticles & MoO_3: NiO nanocomposite were measured by UV-Vis diffuse reflectance spectroscopy as shown in the inset of figure 5(a-c). The bandgap was estimated from Tauc plot, $(F(R)\ h\upsilon)^{1/2}$ vs. the energy of photon ($h\upsilon$).

$$F(R) = \frac{(1-R)^2}{2R} \qquad (2)$$

Kubel-Ka-Munk function (F(R)) is calculated using the relation shown in equation 2 by analyzing the UV-Vis spectroscopy results where R is the reflectance (%) [30]. The bandgap are calculated to be 3.17eV, 4.40eV & 3.66eV respectively which matches well with the reported semiconductor bandgap. It can be attributed to the intrinsic bandgap absorption of the synthesized nanocomposites since all the samples are direct bandgap materials.

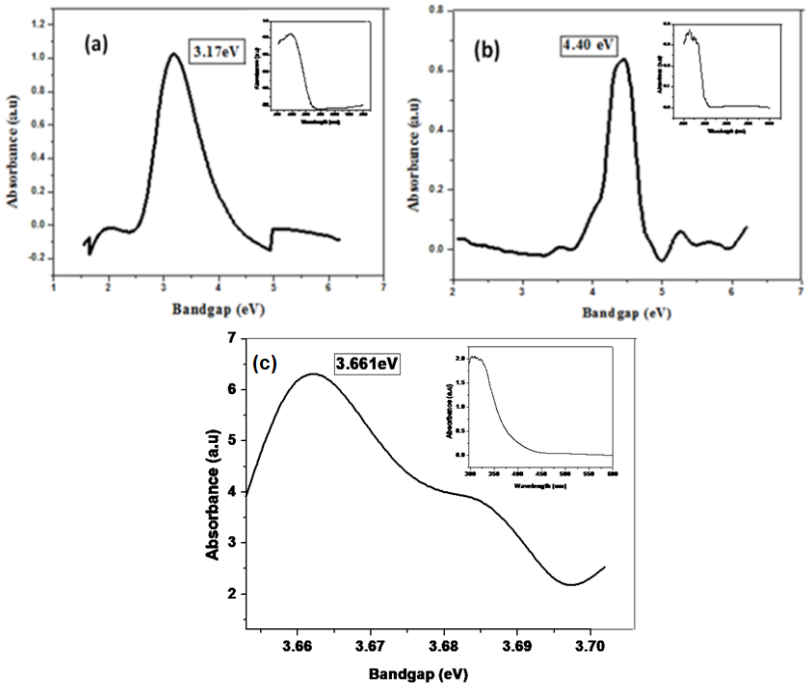

Fig. 5 Tauc plots & UV-DRS spectra of (a) MoO_3 (b) MN & (c) MNA nanocomposites

F. X-Ray Photo-electron Spectroscopy (XPS)

The XPS spectra of Mo, O, Ni & MNA nanoparticles are given in figure 6(a-d). Figure 6(a) shows Mo3d core level spectrum which reveals the spin orbit splitting of $Mo3d_{3/2}$ ground state to be 265.19eV while $Mo3d_{5/2}$ excited state is observed at 277.48eV which is attributed to Mo^{+6}. At 533.05eV in figure 6(b) the broadband observed is attributed to O-1s spectrum. Two peaks centered at 864.55eV and 864.87eV is assigned to $Ni2P_{3/2}$ and $Ni2P_{1/2}$ respectively as shown in figure 6(c). The Ag Spectrum shows two peaks due to spin orbit splitting i.e., $Ag3d_{5/2}$ and $Ag3d_{3/2}$ at 366.82eV and 378.01eV as seen in figure 6(d).

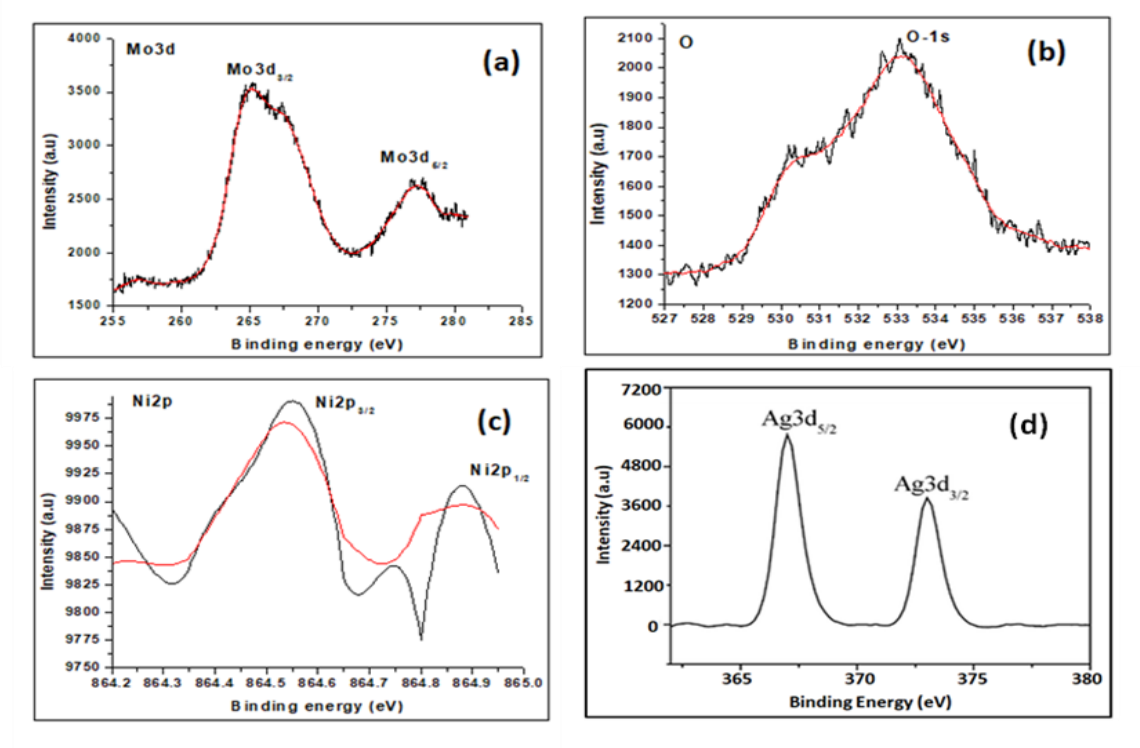

Fig. 6 XPS spectra of (a) Mo (b) O (c) Ni & (d) Ag

VI. GAS SENSING CHARACTERISTICS

The gas sensing characteristics of three samples (MoO_3, MN and MNA) nanocomposites were investigated as a function of operating temperature, different concentrations of CO_2 gas and other interfering gases. The changes in the conductivity of the sensor resulting from the interaction with gas molecules are measured as signals.

Optimization of the operating temperature is crucial for establishing high sensitivity of the sensor towards the target gas which reveals the sensor response as a function of operating temperature. MoO_3 sensor exhibited low sensitivity to CO_2. In contrast, the observed response of MN sensor has sensitivity of S=80.29% and MNA exhibited higher sensitivity of S=87.64% followed by a decrease with increase in operating temperature as shown in figure 7(a).

The response–recovery characteristic is equally important to evaluate the overall performance of the sensor. The response time (Ts) is the time taken for the sensor to reach 90% of the maximum towards test gas and the recovery time (or decay time (Td)) refers to the time taken by sensor to resume to its original conductivity value. In case of nano MoO_3 and MN based sensor, the response time (Ts) is measured as 50s and recovery time (Td) is 40s respectively whereas for nano MNA based sensor, Ts and Td are measured as 30s and 20s respectively towards 1000ppm of CO_2 gas as seen in figure 7(b).

Figure 7(c) shows a typical response of the samples MoO_3, MN and MNA sensors as a function of different concentrations of CO_2 gas at their respective operating temperatures. It is observed that the sensitivity increased linearly with the increase in CO_2 gas concentration.

The cross sensitivity was evaluated to determine the selectivity of the sensor. Thus sensitivity studies of the samples MoO_3, MN & MNA were measured at their respective optimum operating temperature towards 1000ppm of CO_2 gas along with other interfering gases: H_2, ammonia (NH_3), ethanol (ETOH), methanol (MeOH), and LPG. Figure 7(d) represents the resulting data which shows that MNA is highly selective to CO_2 gas comparatively.

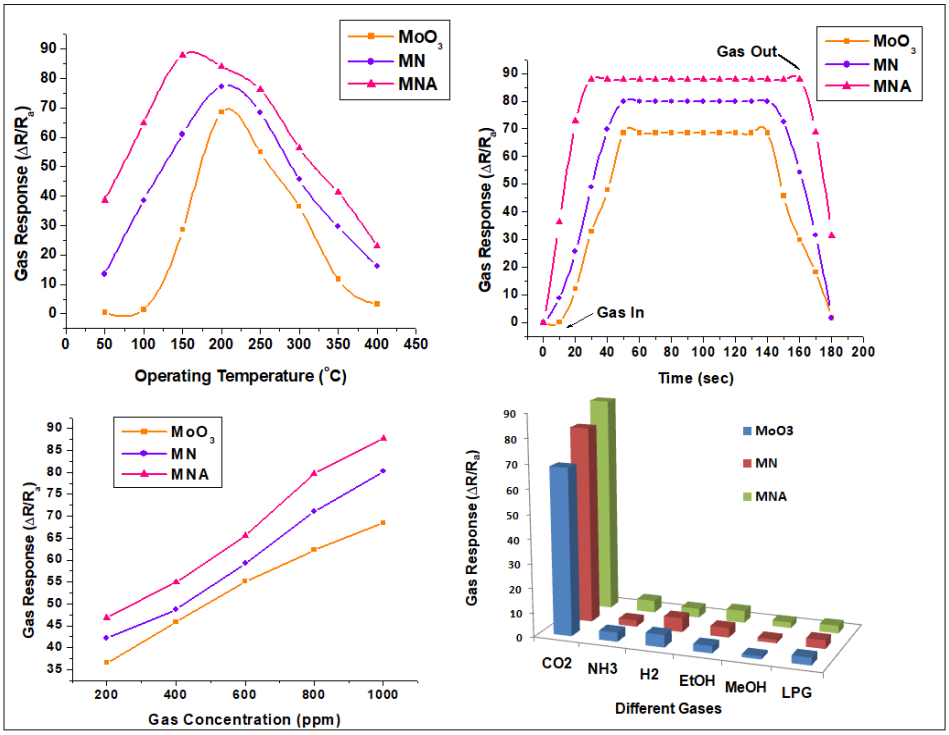

Fig. 7 Gas sensing characteristics of nano MoO_3, MN & MNA – Gas response as a function of (a) Operating Temperature (b) Time response (c) Gas concentrations &

(d) Different interfering gases

VII. GAS SENSING MECHANISM

With reference to our studies we proposed a plausible gas sensing mechanism based on adsorption – desorption mechanism. Oxygen molecules are adsorbed on the MNA surface through two mechanisms: Physisorption and Chemisorption. At low temperature the oxygen molecules are physisorbed on the sensor surface and the bond is weak, leading to a comparatively small response to CO_2 gas. As the temperature increases, the bond between chemisorbed oxygen ions and MNA surface strengthens. The oxygen species dissociate into more active molecules and atomic ions as follows, [15]

$$O_2 \text{ gas} <\!\!\longrightarrow O_2 \text{ ads} + e^- <\!\!\longrightarrow O_2 \text{ ads}^- + e^- (KT) \leftrightarrow O\text{ads}^- + e^- (KT) \leftrightarrow O^{2-} \qquad (3)$$

where O_2 gas is a gaseous oxygen molecule in an ambient atmosphere. The ionization of oxygen molecules occurs due to the capture of electrons from the conduction band of MNA. These oxygen molecules act as electron acceptors, resulting in a deep electron depletion region with reduced electron mobility near the surface of oxide as shown in figure 8. This phenomenon enhances the surface potential and work function.

When the sensor is exposed to air, O_2 adsorbed on the MoO_3: NiO: Ag (MNA) surface traps electrons from the conduction band of MNA due to strong electro negativity of the oxygen atom, and produce adsorbed oxygen O_2^{n-} (ads) as shown in equation (3). Therefore, the concentration of electrons in the conduction band would decrease and the resistance of the material increases. Later when the sensor is exposed to CO_2 atmosphere, the gas molecules react with the adsorbed oxygen species. A chemical redox reaction occurs between CO_2 and O_2^{n-} (ads), which has relatively strong activation on the surface of MNA nanocomposite. Electrons produced from this redox reaction decreases the resistance of the material thus there is an increase in the sensitivity, as the redox reaction is exothermic and results in fast desorption of produced CO_3^{2-} ions from the surface. The released CO_3^{2-} reduces the depletion region, resulting in decrease in the resistance of the sensor. When the MNA sensor is exposed to the air ambient again, the depletion region will be rebuilt by adsorbed oxygen species and the sensor regains its initial resistance.

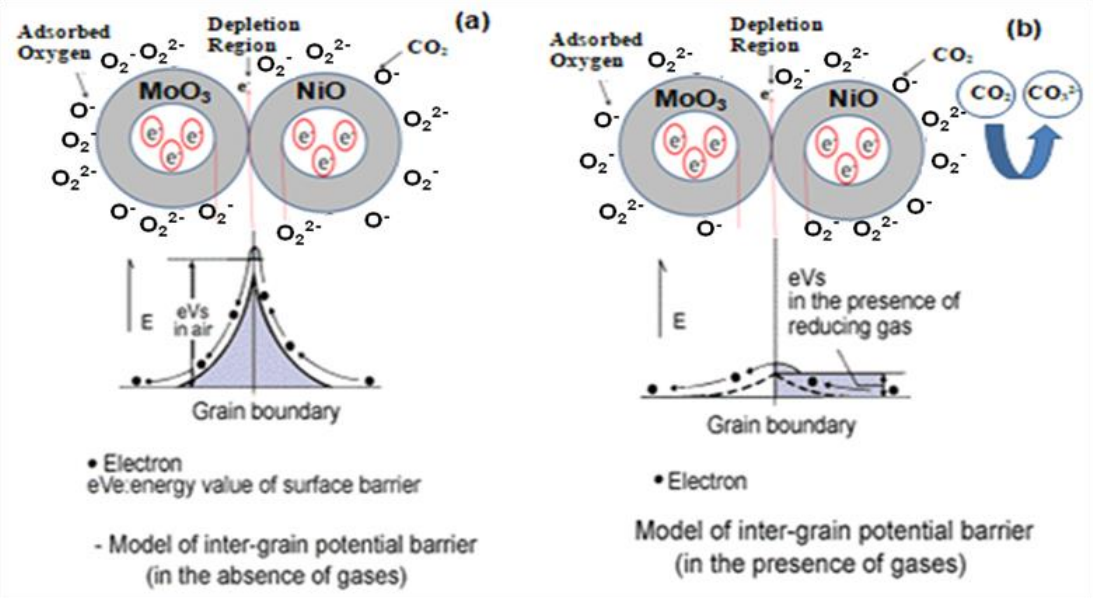

Fig. 8 Gas Sensing Mechanism (a) In absence and (b) In presence of CO_2 gas

VIII. CONCLUSION

The obtained results showed that the MN nanocomposite has a particle size of ~24.5nm exhibiting

the sensitivity of S=80.29% at an optimum temperature of 200^{o}C whereas the MoO_3: NiO: Ag (22nm) shows higher sensitivity of S=87.6% towards 1000ppm CO_2 gas at a low operating temperature of 150^{o}C and selective to CO_2 gas compared to other interfering gases. This proved that the present material (MNA) is highly sensitive and selective to CO_2 gas demonstrating the potential for developing stable and sensitive gas sensor.

CONFLICT OF INTEREST

Authors have no conflict of interest.

ACKNOWLEDGMENT

Authors gratefully acknowledge DST-IDP (GAP 0262), for financial assistance and P.S. P Reddy is thankful to DST (GAP 0262), for project assistantship throughout the research work. M.V. Manasa is thankful to DST-INSPIRE Fellowship grant (GAP 0526).

REFERENCES

[1] A. Star, D.W. Steuerman, J.R. Heath, J.F. Stoddart, "Dispersion and solubilization of single-walled carbon nanotubes with a hyperbranched polymer", Angew. Chem. Int. Ed., 41, 2508, 2002.
[2] Joseph J. Suter, JohnsHopkins, "Sensors and sensor systems research and development at ApL with a View toward the Future", ApL Technical Digest, 26, 4, 2005.
[3] Francisco Márquez, Carmen Morant, "Nanomaterials for Sensor Applications", Soft Nanoscience Letters, 5, 1-2, 2015.
[4] Shao Su, Wenhe Wu, Jimin Gao, Jianxin Lu and Chunhai Fan, "Recent Trends in Nanomaterials Applications in Environment", J. Mater. Chem., 22, 18101, 2012.
[5] Zhiyu Wang, Srinivasan Madhavi, and Xiong Wen (David) Lou, "Ultra long α-MoO_3 Nanobelts: Synthesis and Effect of Binder Choice on their Lithium Storage Properties", J. Phys. Chem. C, 116, 12508−12513, 2012.
[6] Sumistha Das, Biswarup Sen, Nitai Debnath, "Nanomaterials-based sensors for applications in environmental monitoring", Environmental Science and Pollution Research, 22, 23, 18333-18344, 2015.
[7] Joseph J. BelBruno, "Nanomaterials in Sensors", Nanomaterials, 3, 572-573, 2013.
[8] Liqiang Mai, Fan Yang, Yunlong Zhao, Xu Xu, Lin Xa, Bin Ha, Yanzhu Luo and Hangyu Liu, "Molybdenum oxide nanowires: synthesis & properties", Mater. Today, 14, 7-8, 2011.
[9] Arnab Ganguly, Raji George, "Synthesis, characterization and gas sensitivity of MoO_3 nanoparticles", Bulletin of Materials Science, 30, 2, 183–185, 2007.
[10] Arumugam Manivel, Gang-Juan Lee, Chin-Yi Chen, Jing-Heng Chen, Shih-Hsin Ma, Tzzy-Leng Horng, Jerry J. Wu, "Synthesis of MoO_3 nanoparticles for azo dye degradation by catalytic ozonation", Mat. Res. Bul., 62, 184-191, 2015.
[11] N. Serpone, P. Maruthamuthu, P. Pichat, E. Pelizzetti, H. Hidaka, "Exploiting the interparticle electron transfer process in the photocatalysed oxidation of phenol 2-chlorophenol and pentachlorophenol: chemical evidence for electron and hole transfer between coupled semiconductors", Journal of Photochemistry & Photobiology A: Chemical, 85, 247-255, 1995.
[12] A. Hernandez, L. Maya, E.S. Mora, E.M. Sanchez, "Sol-gel synthesis, characterization and photocatalytic activity of mixed oxide ZnO-Fe_2O_3", Journal of Sol-Gel Science and Technology, 42, 71-78, 2007.
[13] J. Rabani, "Sandwich colloids of zinc oxide and zinc sulfide in aqueous solutions", Journal of Physical Chemistry, 93, 7707-7713, 1989.
[14] M.K. Kumar, S. Ramaprabhu, "Nanostructured Pt functionalized multiwalled carbon nanotube based hydrogen sensor", Journal of Physical Chemistry B, 110, 11291-11298, 2006.

[15] Arumugam Manivel, Gang-Juan Lee, Chin-Yi Chen, Jing-Heng Chen, Shih-Hsin Ma, Tzzy-Leng Horng, Jerry J. Wu, "Synthesis of MoO3 nanoaparticles for azo dye degradation by catalytic ozonation", Mat. Res. Bul. 62, 184-191, 2015.
[16] R. Ahuja, L. Fast, O. Eriksson, J.M. Wills, B. Johansson, "Elastic and High Pressure Properties of ZnO", Journal of Applied Physics, 83, 8065-8067, 1998.
[17] M.D. Driessen, V.H. Grassian, "Photooxidation of trichloroethylene on Pt/TiO_2", Journal of Physical Chemistry B, 102, 1418-1423, 1998.
[18] A. Fujishima, K. Honda, Electrochemical photolysis of water at a semiconductor electrode, Nature, 238, 37-38, 1972.
[19] T. Hisanaga, K. Harada, K. Tanaka, "Photocatalytic degradation of organochlorine compounds in suspended TiO_2", Journal of Photochemistry & Photobiology A: Chemical, 54, 113-118, 1990.
[20] P.S. Prasad Reddy, K. Sreenivasa Reddy, B. Adi Narayana Reddy, M.V. Manasa, G. Sarala Devi and G. Nageswara Rao, "Gas Sensing Characteristics of ZnO: Nb_2O_5 Nanocomposite towards Hydrogen Gas", Journal of Advanced Physics, 6, 418-421, 2017.
[21] R. Kocache, "Evaluation and Applications of Gas Sensors", Sensor Review, 14, 8-12, 1994.
[22] K. Obata, S. Kumazawa, K. Shimanoe, N. Miura, N. Yamazoe, "Potentiometric Sensor based on Nasicon and In_2O_3 for detection of CO_2 at room temperature - Modification with foreign substances", Sensors and Actuators B, 76, 639-643, 2001.
[23] H. Nanto, H. Sokooshi, T. Kawai, T. Usuda, "Zinc oxide thin-film trimethylamine sensor with high sensitivity and excellent selectivity", Journal of Materials Science Letters, 11, 235-237, 1992.
[24] E.A. Meulenkamp, "Synthesis and growth of ZnO nanoparticles", Journal of Physical Chemistry B, 102, 5566-5572, 1998.
[25] G.K. Mor, M.A.Carvalho, O.K. Varghese, M.V. Pishko, C.A. Grimes, "A room-temperature TiO_2-nanotube hydrogen sensor able to self-clean photoactively from environmental contamination", Journal of Materials Research, 19, 628-634, 2004.
[26] J.H. Yuan, K. Wang, X.H. Xia, "Highly ordered platinum-nanotubule arrays for amperometric glucose sensing", Advanced Functional Materials, 15, 803-809, 2005.
[27] A.B. Kashyout, M. Soliman, M. El Gamal, M. Fathy, "Preparation and characterization of nano particles ZnO films for dye-sensitized solar cells", Materials Chemistry and Physics, 90, 230-233, 2005.
[28] S. Anandan, "Photocatalytic effects of titania supported nanoporous MCM-41 on degradation of methylorange in the presence of electron acceptors", Dyes Pigments, 76, 535-541, 2008.
[29] J. Kong, M.G. Chapline, H. Dai, "Functionalized carbon nanotubes for molecular hydrogen sensors", Advanced Materials, 13, 1384-1386, 2001.
[30] Hamoon Hedayat, P. Siva Prasada Reddy, M.V. Manasa, G. Sarala Devi, J.V. Ramana Rao, G. Nageswara Rao, "Nanostructure evolution of zinc stannate: A suitable material for liquefied petroleum gas detection", Journal of Alloys and Compounds, 704, 413-419, 2017.
[31] Joseph J. Suter, "Sensors and sensor systems researchand Development at ApL with a View Toward the Future", Johnshopkins ApL Technical Digest, 26, 4, 2005.
[32] Shao Su, Wenhe Wu, Jimin Gao, Jianxin Lu and Chunhai Fan, "Nanomaterials based sensors for applications in environmental monitoring", J. Mater. Chem., 22, 18101, 2012.
[33] Z.Y. Can, H. Narita, J. Mizusaki, H. Tagawa, "State Detection of Carbon Monoxide", Solid State Ionics, 79, 344-348, 1995.
[34] N.O. Savage, S.A. Akbar, P.K. Dutta, "High temperature potentiometric carbon dioxide sensor with minimal interference to humidity", Sensors and Actuators B, 72, 239-248, 2001.
[35] M.V. Manasa, P.S. Prasada Reddy, B. Adi Narayana Reddy and G. Sarala Devi, "Molybdenum Oxide Nanoparticles: Synthesis, Characterization and Application in Green-House Gas Sensing", Journal of Advanced Physics, 7, 1-7, 2018.

Authors Biography

M.V. Manasa holds B.Tech. (Electronics & Communication Engineering) & M.Tech. (Nano Technology – goldmedalist) degrees from Jawaharlal Nehru Technological University, Hyderabad. She worked on synthesis, characterization and simulation of high-K dielectric materials, nano lanthanides and MOSFET simulation studies. She has several papers in international journals and a book in her credit. She was awarded with DST-INSPIRE fellowship for pursuing Ph.D. and presently working at CSIR-Indian Institute of Chemical Technology (CSIR-IICT). Her present research is oriented towards development of green house gas sensors via semiconductor nanomaterials.

Dr. G. Sarala Devi received her M.Phil degree from Hyderabad Central University (HCU), Ph.D. from Indian Institute of Chemical Technology (IICT) - Hyderabad and Post Doc. from Nagasaki University – JAPAN. She is a recipient of 10 prestigious awards few to mention, BOYSCAST fellow- Japan, DAAD – Germany, DST Young Scientist travel grant, Max Planck Fellow - Germany, Research excellence award, Technology award, Distinguished Scientist award, etc.

Presently she is a Principal Scientist, at Indian Institute of Chemical Technology, Hyderabad - India. Research focuses on Applied & Basic Research in the field of Materials Science - Nanomaterials, composites, biomaterials, conducting polymers, semiconductor nanomaterials etc. with multifunctional properties tailored to suit applications in several areas of catalysis, Chemical Sensors - MEMS and NEMS and biological applications.

Dr. P. S. Prasada Reddy received his M,Tech. in NanoTechnology from Karunya University- Coimbatore. He completed his Ph.D.in Material Science at CSIR - Indian Institute of Chemical Technology (CSIR-IICT). His current research interest is in the area of Nanomaterials and Nanocomposites, Semiconducting Metal, Metal oxides for application in MEMS and NEMS technology. Presently he is working as Associate Professor in Physics at Dr. B.R. Ambedkar University, Andhra Pradesh, India.